REFERENCES

[1] S.G. Johnson and J.D. Joannopoulos. Introduction to photonic crystals: Bloch's theorem, band diagram, and Gap (but no defects). Available from: http://ab-initio.mit.edu (accessed January, 2006).

[2] A. Yamilov, et.al. Photonic band structure of ZnO photonic crystal slab laser. Journal of Applied Physics. 98, 103102 (2005).

[3] B.P. Hiett, et.al. Application of finite element methods to photonic crystal modeling. IEE Proc.-Sci. Meas. Technol., 149, 5,(2002).

[4] J.D. Shumpert. Modeling of periodic dielectric structures (Electromagnetic crystals). A dissertation submitted in partial fulfillment of the requirements for the degree of Doctor of Phylosophy (Electrical Engineering), The University of Michigan, 2001.

[5] X. L. Yang, et.al. Theoretical bandgap modeling of two-dimensional triangular photonic crystals formed by interference technique of three noncoplanar beams. OPTICS EXPRESS 1053, 11, 9, (2003).

[6] B.P. Hiett, et.al. Photonic band gaps in 12-fold symmetric quasycrystals. Journal of Material Science: Materials in Electronics. 14 (2003): 413-416.

[7] Chin-ping Yu and Hung-chun Chang. Compact finite-difference frequency-domain method for the analysis of two-dimensional photonic crystals. OPTICS EXPRESS 1397, 12, 7 (2004).

[8] W. Axmann and P. Kuchment. An efficient finite element method for computing spectra of photonic and acoustic band gap materials I. Scalar case. Journal of Computational Physics. 150 (1999): 468-481.

[9] F. Cuesta-Soto, et.al. All-optical switching structure based on a photonic crystal directional coupler. OPTICS EXPRESS 161. 12, 1 (January 2004).

[10] C. Kittel. Introduction to Solid State Physics, 7th edition. John Wiley&Sons, Inc., 1996.

[11] J.F. DeFord, et.al. Periodic boundary conditions in the parallel eigensolver OM3P: Application of the inexact Lanczos process ti Hermitian systems. Proceedings of the 2003 Particle Accelerator Conference (2006).

[12] Kenji K. and Tsutomo K. Introduction to optical waveguide analysis, solving Maxwell's equations and the Schrodinger's equations. John Wiley & Sons, Inc., 2001.

[13] N. Sukumar and A. Tabarei. Conforming polygonal finite elements. International Journal for Numerical Methods in Engineering. 61 (2004): 2045-2066.

[14] Giuseppe Pelosi, et.al. Quick finite elements for electromagnetic waves. Artech House, Inc., Boston, London, 1998.

[15] Jianming Jin. The finite element method in electromagnetics. John Wiley & Sons, Inc., 1993.

[16] Mark Meyer, et.al. Generalized barycentric coordinates on irregular polygons. Journal of Graphic Tools. 7, 1 (2002): 13-22.

[17] Kai Hormann. Barycentric coordinates for arbitrary polygons in the plane. Technical Report No. 5, Institute of Computer Science, Clausthal University of Technology, Germany. (2005).

[18] N. Sukumar and E.A. Malsch. Recent advances in the construction of polygonal finite element interpolants. Arhcives of Computational Methods in Engineering. 13, 1 (2006): 129-163.

[19] Joe Warren, et.al. Barycentric coordinates for convex sets. Advances in Computational and Applied Mathematics. (2005).

[20] Michael S. Floater, et.al. A general construction of barycentric coordinates over convex polygons. Available at: http://www2.in.tuclausthal.de (accessed August, 2006).

[21] N. Sukumar and A. Tabarrei. Numerical formulation and application of polygonal finite elements", 7th International ESAFORM Conference on Material Forming, Trondheim, Norway (2004).

[22] Paras N. P. Nanophotonics. John Wiley&Sons, Inc., 2004

[23] B.P. Hiett, et.al. Photonic band gaps in 12-fold symmetric quasicrystals. Journal of Material Science: Materials in Electronics. 14 (2003): 413-416.

[24] R.D. Cook, et.al. Concept and application of finite element analysis, 4th edition. John Wiley&Sons, Inc., 2002.

[25] Rao V.G. and Mikhail J.S. Polygonal surface mesh optimization. Engineering with Computers, 20 (2004): 265-272.

[26] M.H. Shih, et.al. Two-dimensional photonic crystal Mach-Zehnder interferometers. Applied Physics Letters. 84, 4 (2004).

[27] D.M. Tennant, et.al. Fabrication methods for a quantum cascade photonic crystal surface emitting laser. J. Vac. Sci. Technol. B. 21, 6 (2003).

[28] Timo Euler, et.al. Polygonal Finite Elements. IEEE Transactions on Magnetics. 42, 4 (April 2006).

[29] K.Srinivasan.Semiconductor Optical Microcavities for Chip-Based Cavity QED. Available at: http://etd.caltech.edu (accessed on 20 February 2007).

[30] Marco L. Design and fabrication of silicon photonic crystal optical waveguide. Journal of Lightwave Technology. 18, 10 (October, 2000)

[31] -. Nanofabrication Facility. Available at: http://www.ampel.ubc.ca/nanofab (accessed on 20 February 2007)

[32] Tirupathi R.C. and Ashok D.B. Introduction to Finite Elements in Engneering, 3rd edition. International Edition, Prentice Hall, Inc., 2002.

[33] J.E. Akin. Finite element analysis with error estimators. Elsevier Butterworth-Heinemann, 2005.

[34] D.S. Burnett. Finite Element Analysis, From Concept to Applications. Addison-Wesley Publishing Company, 1987.

[35] Ming-Chieh Lin and Ruei-Fu Jao. Finite element analysis of photon density of states for two-dimensional photonic crystals with in-plane light propagation. OPTICS EXPRESS 207, 15, 1 (January 2007).

[36] Xie Juan, et.al. Self-assembled ZnO colloidal photonic crystals: Light channels in cracks. Materials Science in Semiconductor Processing, 9 (2006): 136–140.

[37] Masanori Koshiba. Modeling of Photonic Crystal Fibers. IEEJ Trans. FM., 124, 12(2004).

PUBLICATIONS

1. Eny Sukani Rahayu and Tuptim Angkaew. Finite Element Analysis of 2-Dimensional Photonic Crystal. Proceeding of AUN/Seed-Net Field Wise Seminar on Multimedia Signal Processing and Communication System. (October 16-17, 2006).

2. Eny Sukani Rahayu and Tuptim Angkaew. A Finite Element Method with Polygonal Elements for Analyzing a Band Gap Characteristic of Square Lattice Photonic Crystals. Accepted paper for ECTI-CON 2007 held on May 9-11, 2007.

APPENDIX

APPENDIX A

FIELD DISTRIBUTIONS ON A SQUARE AND A TRIANGULAR LATTICE PHOTONIC CRYSTALS

Using the linear triangular FEM with 31 sample points of wave vectors applied to Mesh I of the square lattice unit cell and Mesh II of the triangular lattice unit cell, the behaviors of the fields on a unit cell are presented by showing field distributions over the unit cell. The field distributions are divided into two types that are obtained from the square lattice and the triangular lattice unit cells. For each type of unit cells, the behaviors of the *E*-fields and *H*-fields are presented as the solutions of TM and TE modes, respectively. Here, the dielectric constant, ε_r, is 8.9 and the ratio between the radius of the rod, r, and the lattice constant, a, is $r/a = 0.2$.

The field distributions in the square lattice unit cell are provided in the real numerical values as well as in the triangular lattice unit cell. The purpose of showing this field distributions is to give more understandings about which parts of the unit cell that give the more fluctuating (higher frequency) fields and less fluctuating (lower frequency) fields and also the relation of FEM formulation to the behaviors of this systems.

A.1 Case of a square lattice unit cell

A.1.1 Field distributions in the real values

With the band gap characteristic obtained as shown in Figure A.1

Figure A.1, the *E*-field and *H*-field distributions over the square unit cell are presented in Figure A.2-A.24. The points marked in Figure A.1 with the black stars are evaluated and their related field distributions are ones plotted in this report.

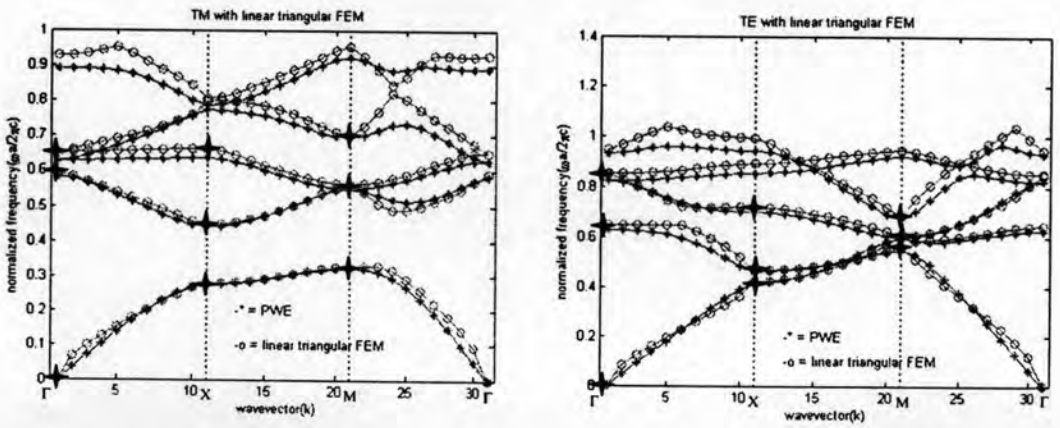

Figure A.1 Band gap characteristics of a square lattice unit cell for TM and TE modes

At Γ_1:

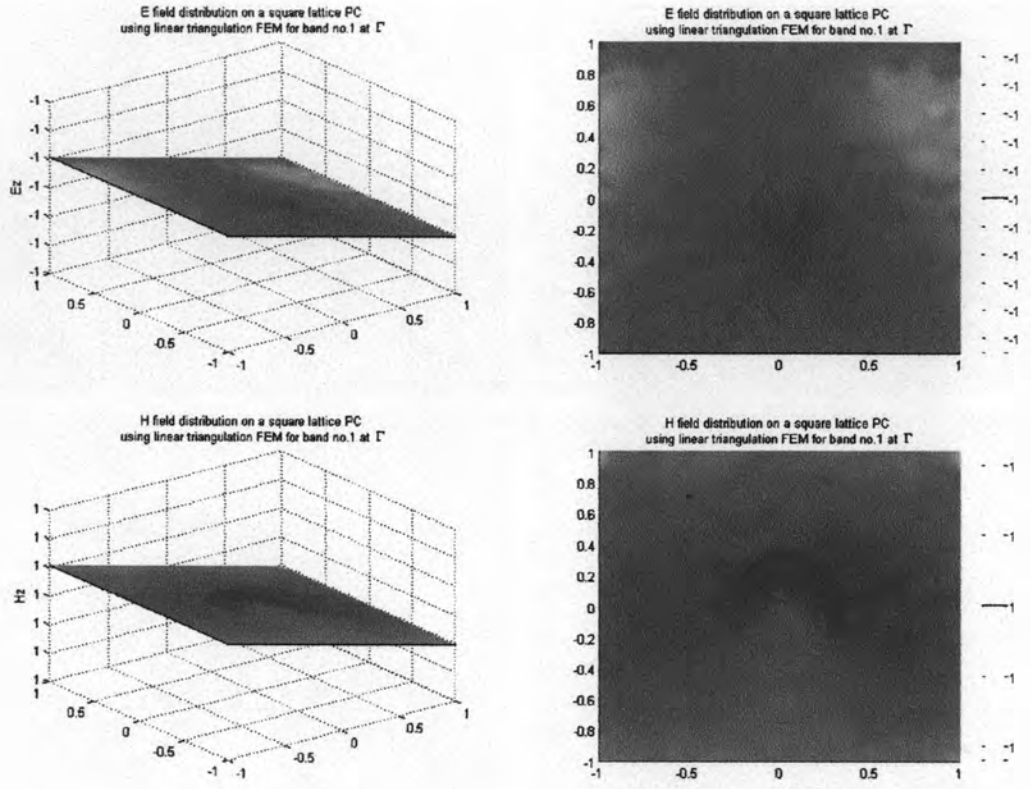

Figure A.2 *E*-field and *H*-field distributions at Γ point for the first band in real values.

At Γ_2:

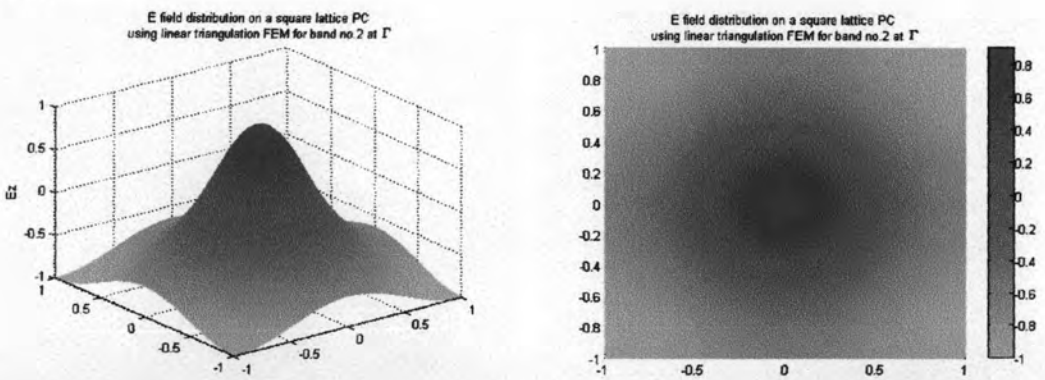

Figure A. 3 *E*-field and *H*-field distributions at Γ point for the second band in real values

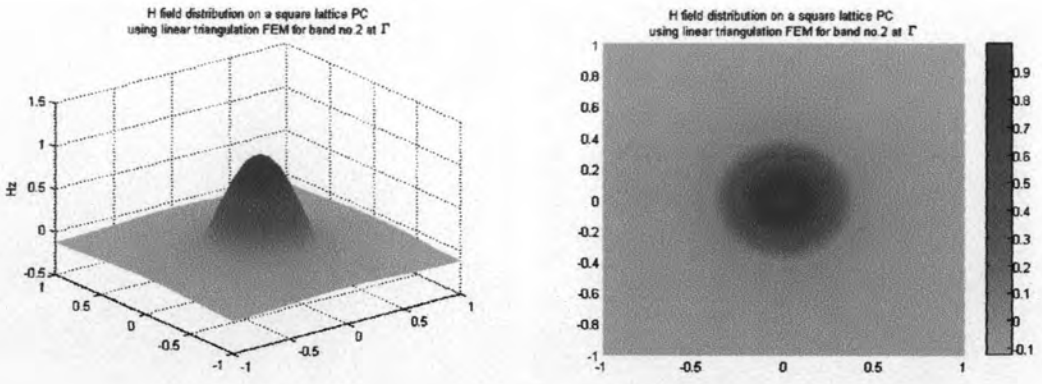

Figure A. 4 *E*-field and *H*-field distributions at Γ point for the second band in real values (cont.)

At Γ_3:

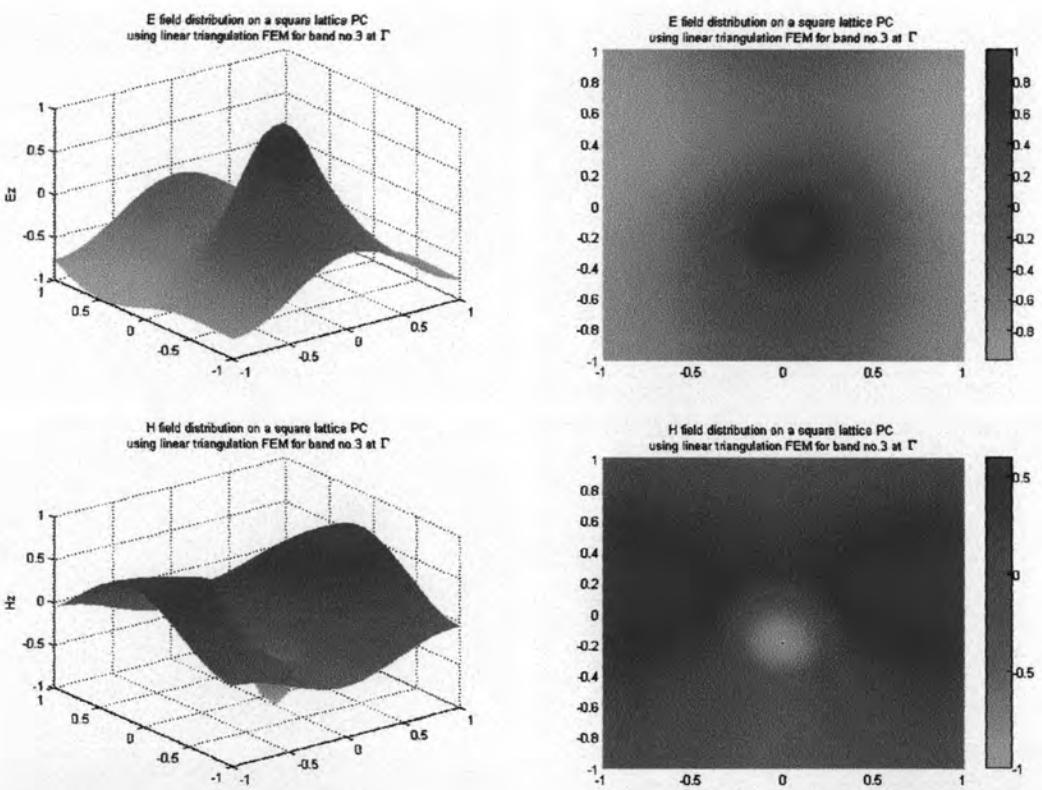

Figure A. 4 *E*-field and *H*-field distributions at Γ point for the third band in real values.

At X_1:

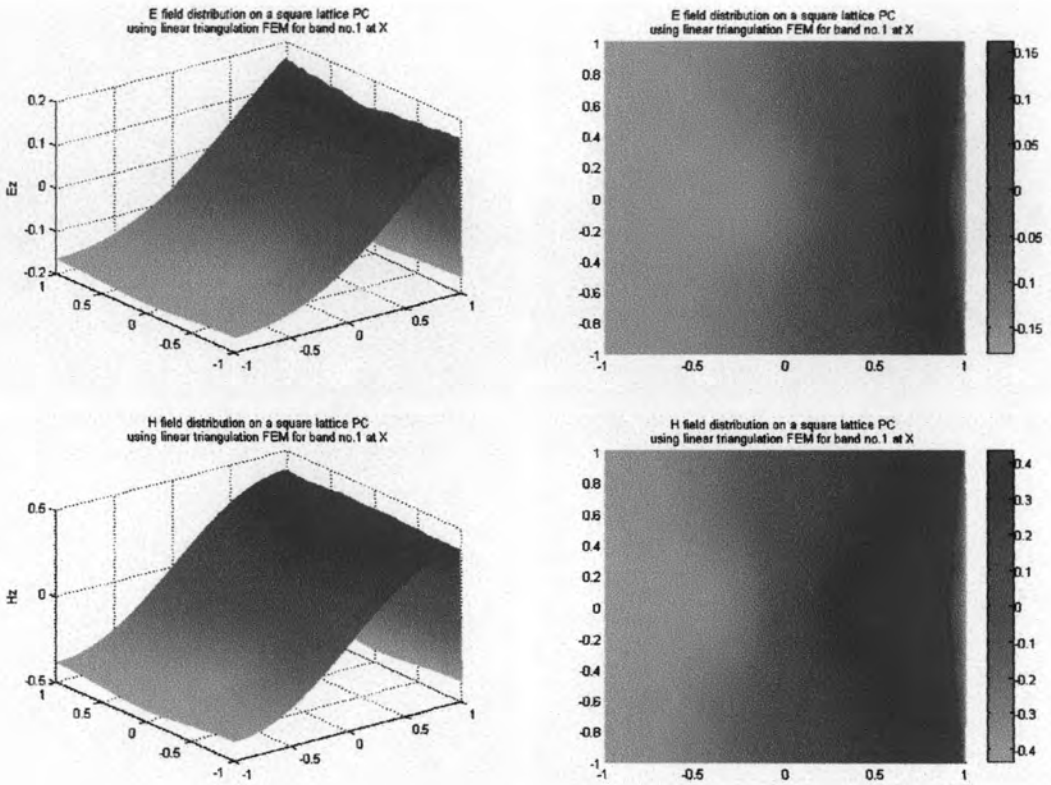

Figure A. 5 E-field and H-field distributions at X point for the first band in real values.

At X_2:

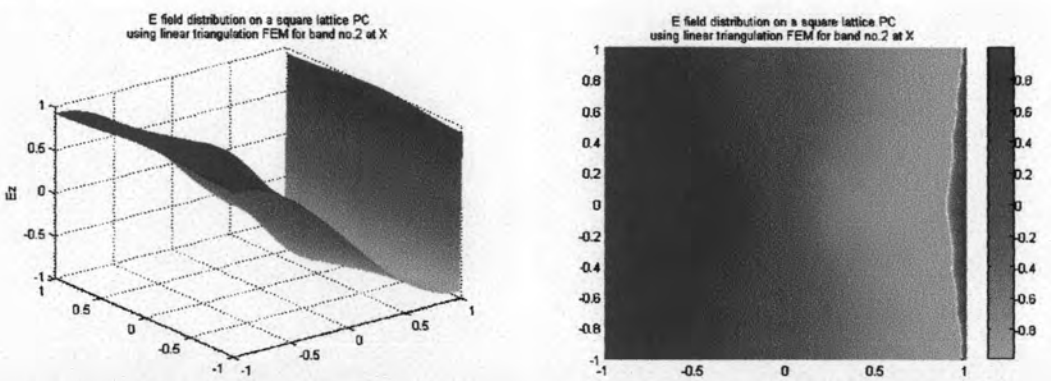

Figure A. 6 E-field and H-field distributions at X point for the second band in real values.

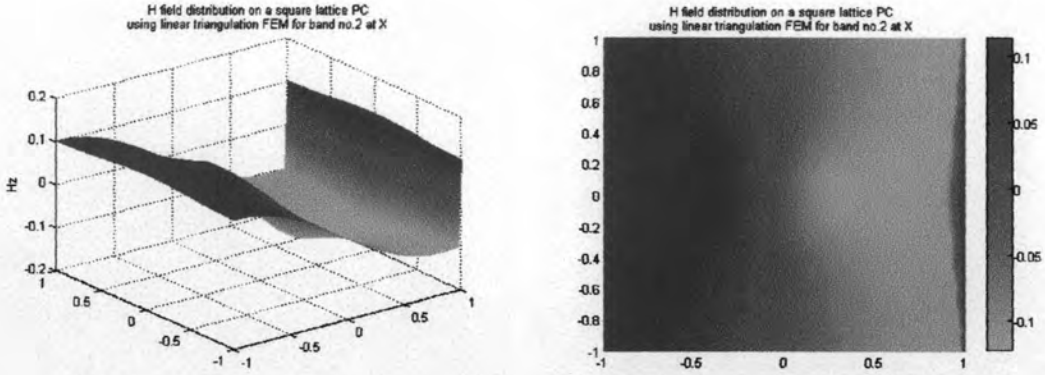

Figure A. 6 E-field and H-field distributions at X point for the second band in real values (cont.).

At X_3:

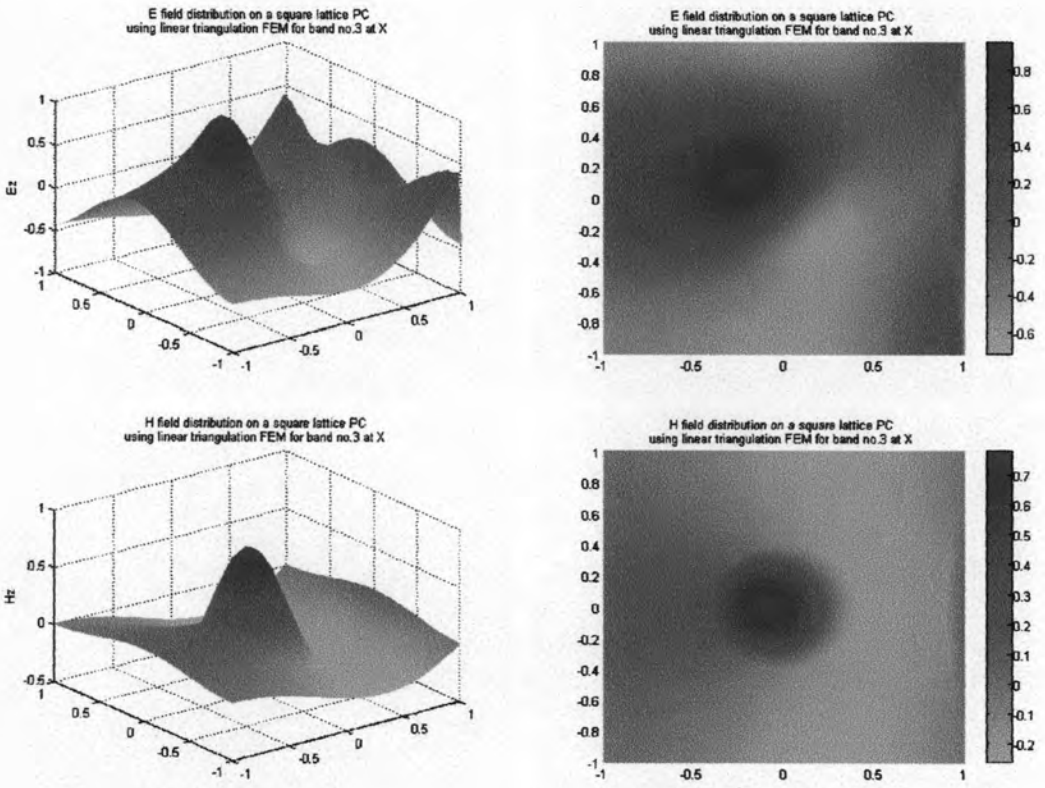

Figure A. 7 E-field and H-field distributions at X point for the third band in real values.

At M_1:

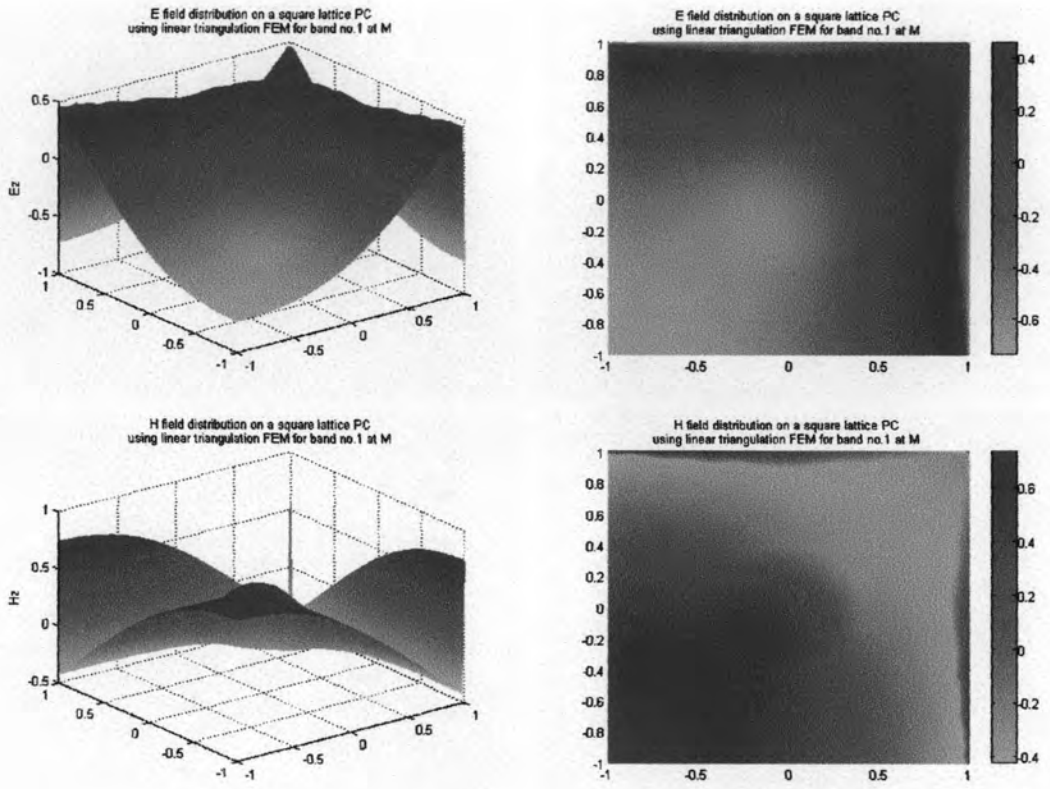

Figure A. 8 E-field and H-field distributions at M point for the first band in real values.

At M_2:

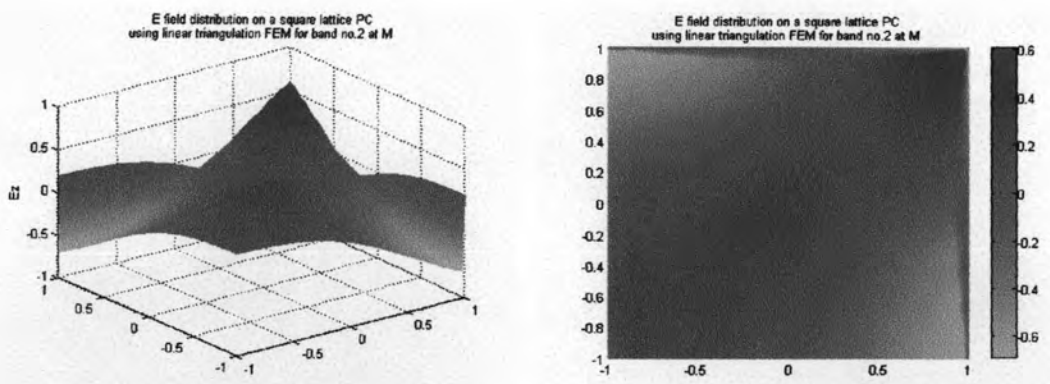

Figure A. 9 E-field and H-field distributions at M point for the second band in real values.

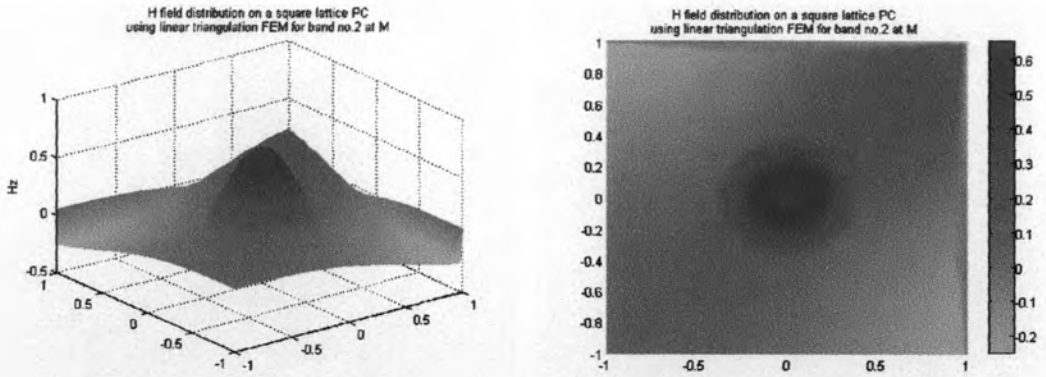

Figure A. 9 E-field and H-field distributions at M point for the second band in real values (cont.).

At M_3:

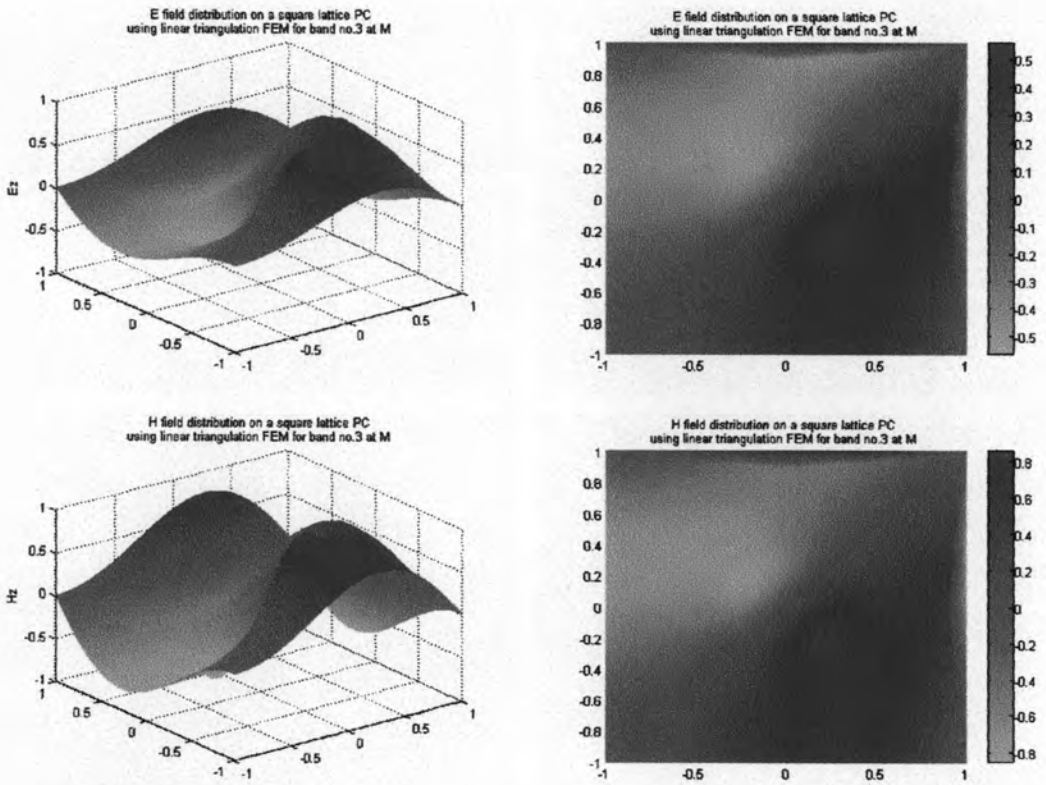

Figure A. 10 E-field and H-field distributions at M point for the third band in real values.

A.2 Case of a triangular lattice unit cell

At Γ_1:

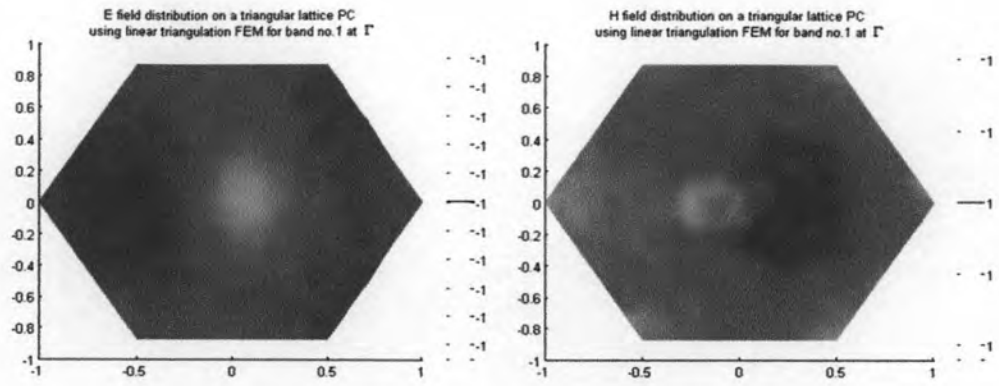

Figure A.5 *E*-field and *H*-field distributions at Γ point for the first band

At Γ_2:

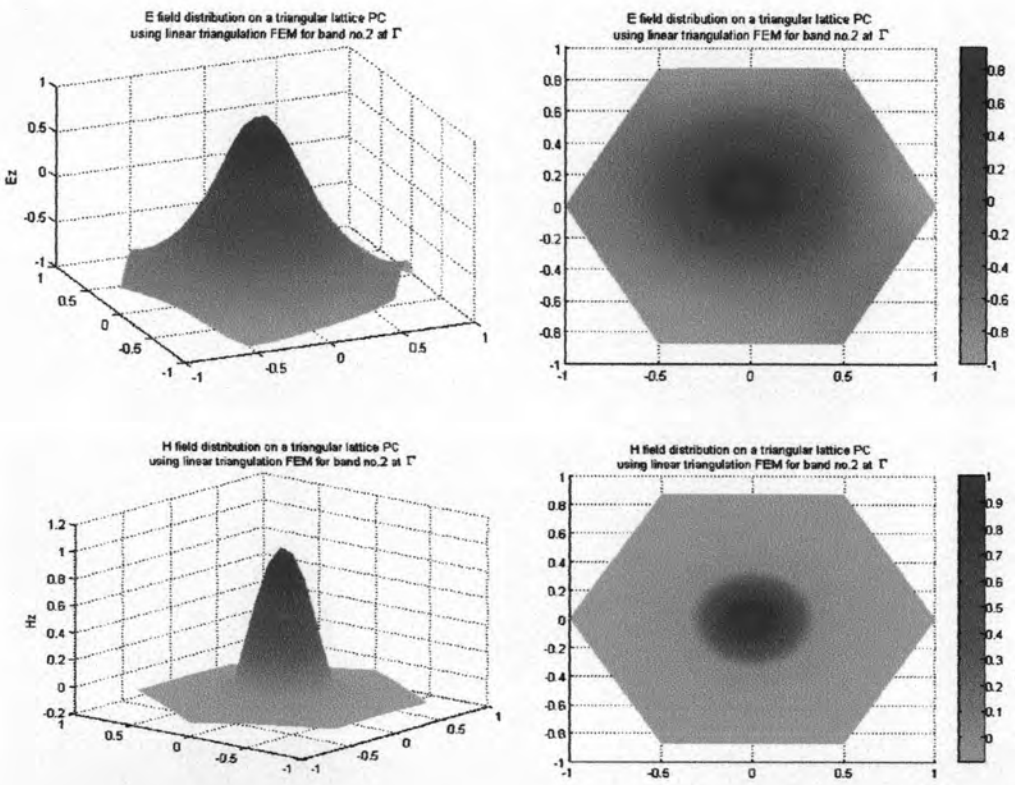

Figure A.6 E-field and H-field distributions at Γ point for the second band

At Γ_3:

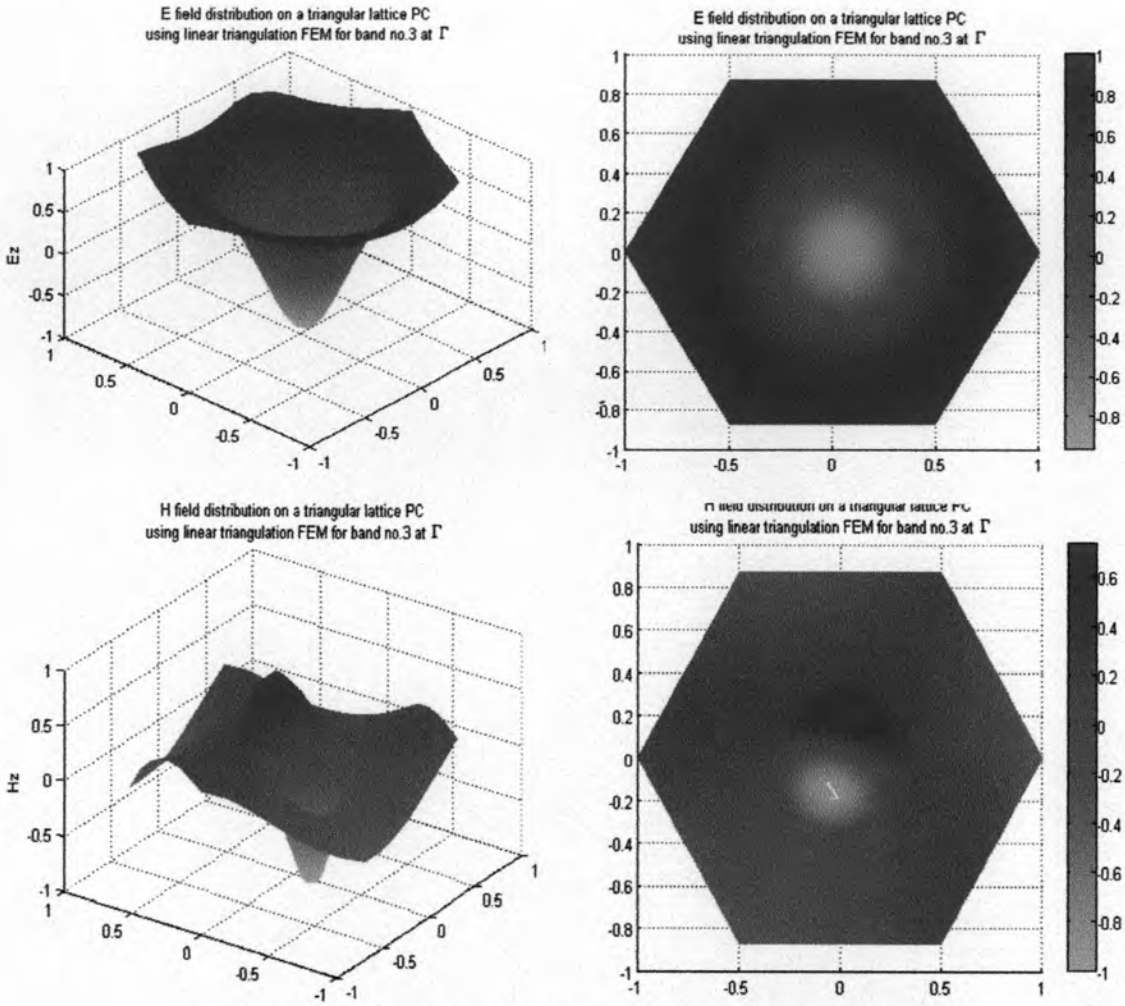

Figure A.7 *E*-field and *H*-field distributions at Γ point for the third band

At X_1:

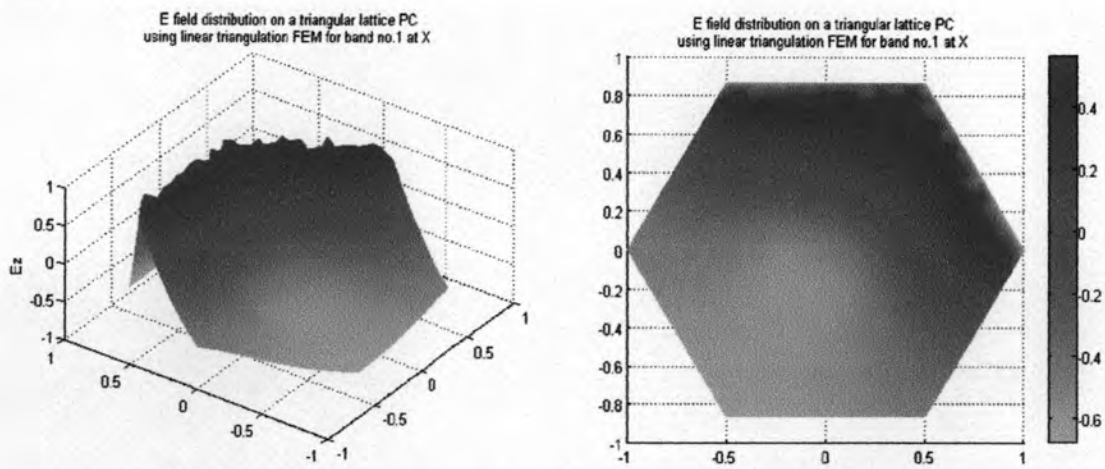

Figure A.8 E-field and H-field distributions at X point for the first band

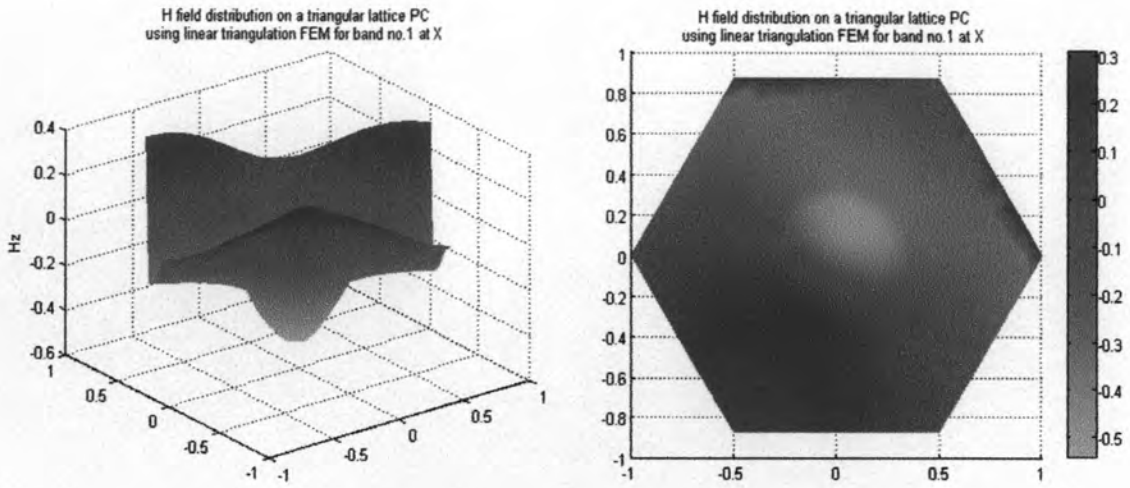

Figure A.9 E-field and H-field distributions at X point for the first band (cont.)

At X_2:

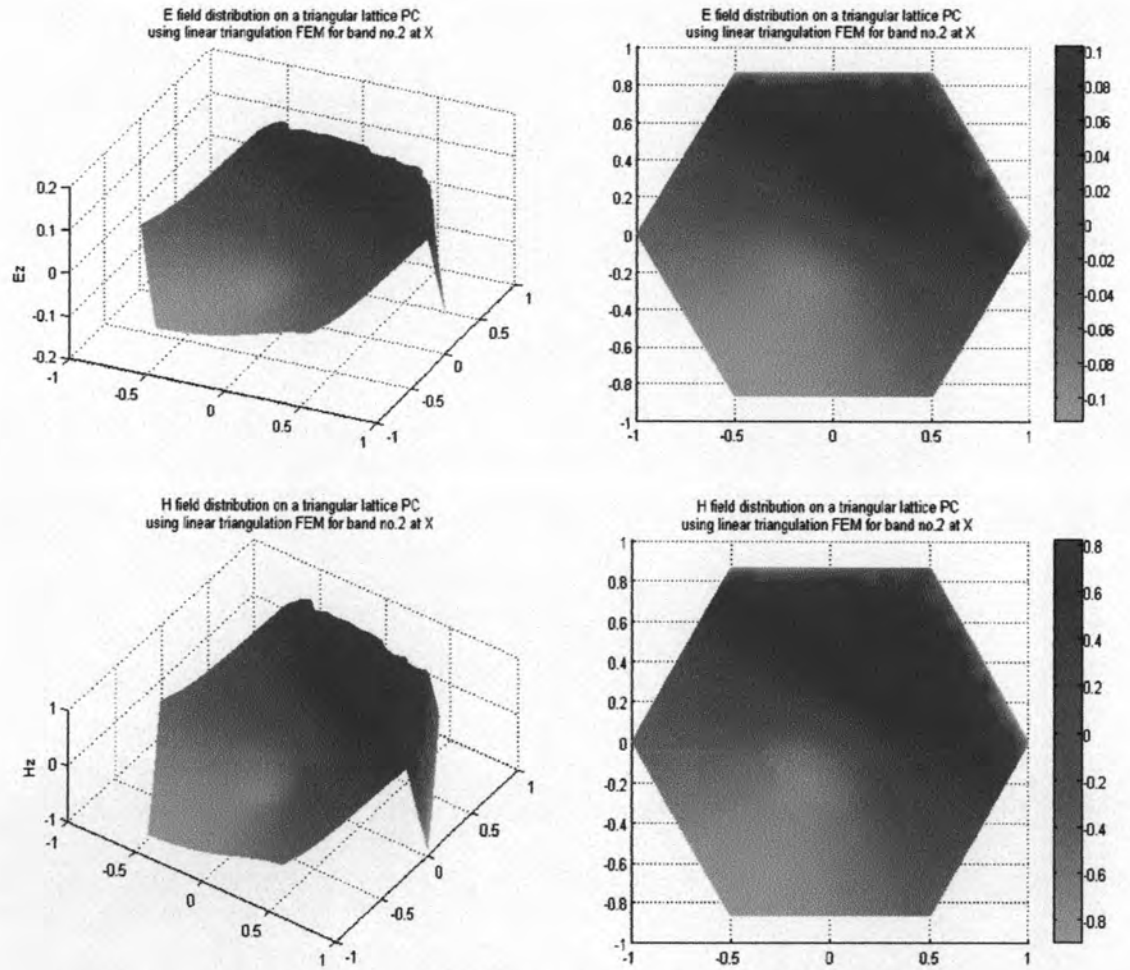

Figure A. 10 E-field and H-field distributions at X point for the second band

At X_3:

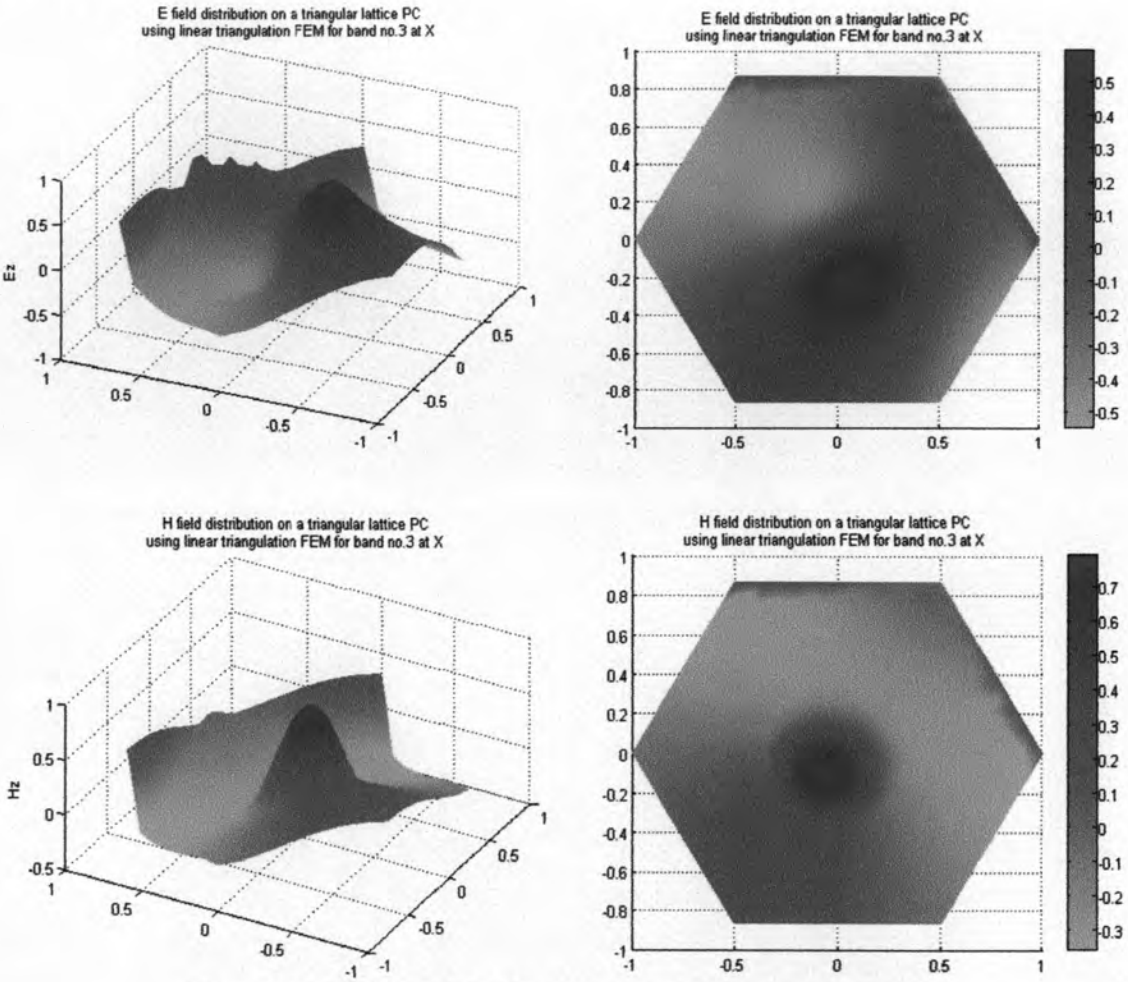

Figure A. 11 E-field and H-field distributions at X point for the third band

At M_1:

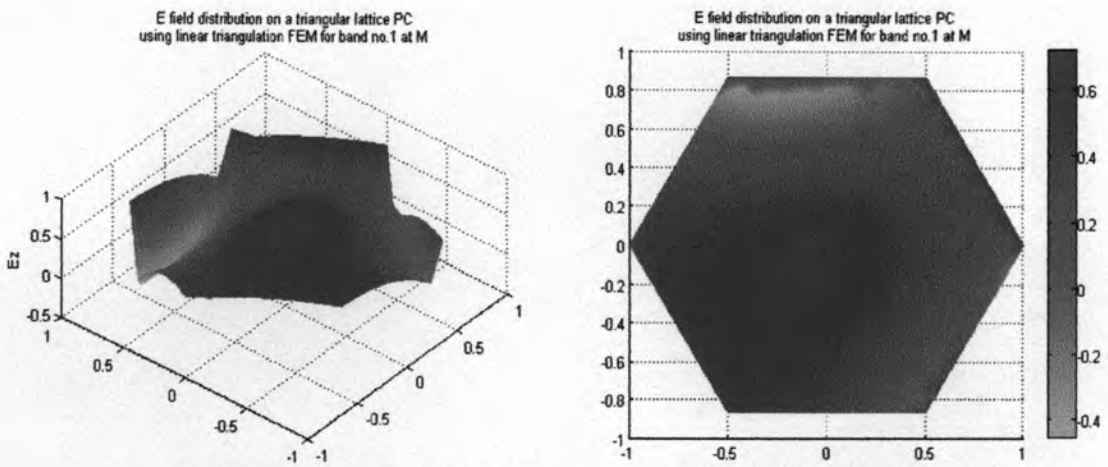

Figure A. 12 *E*-field and *H*-field distributions at M point for the first band

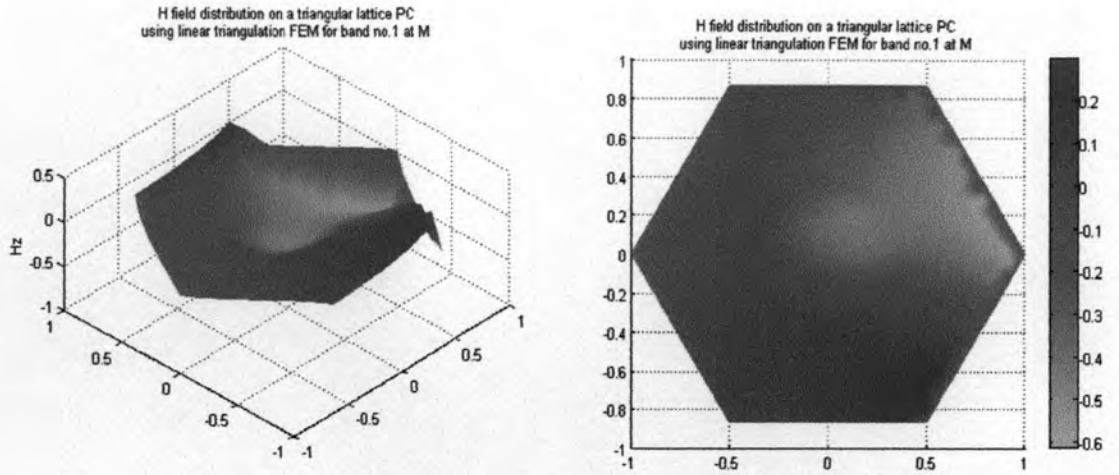

Figure A. 13 *E*-field and *H*-field distributions at M point for the first band

At M_2:

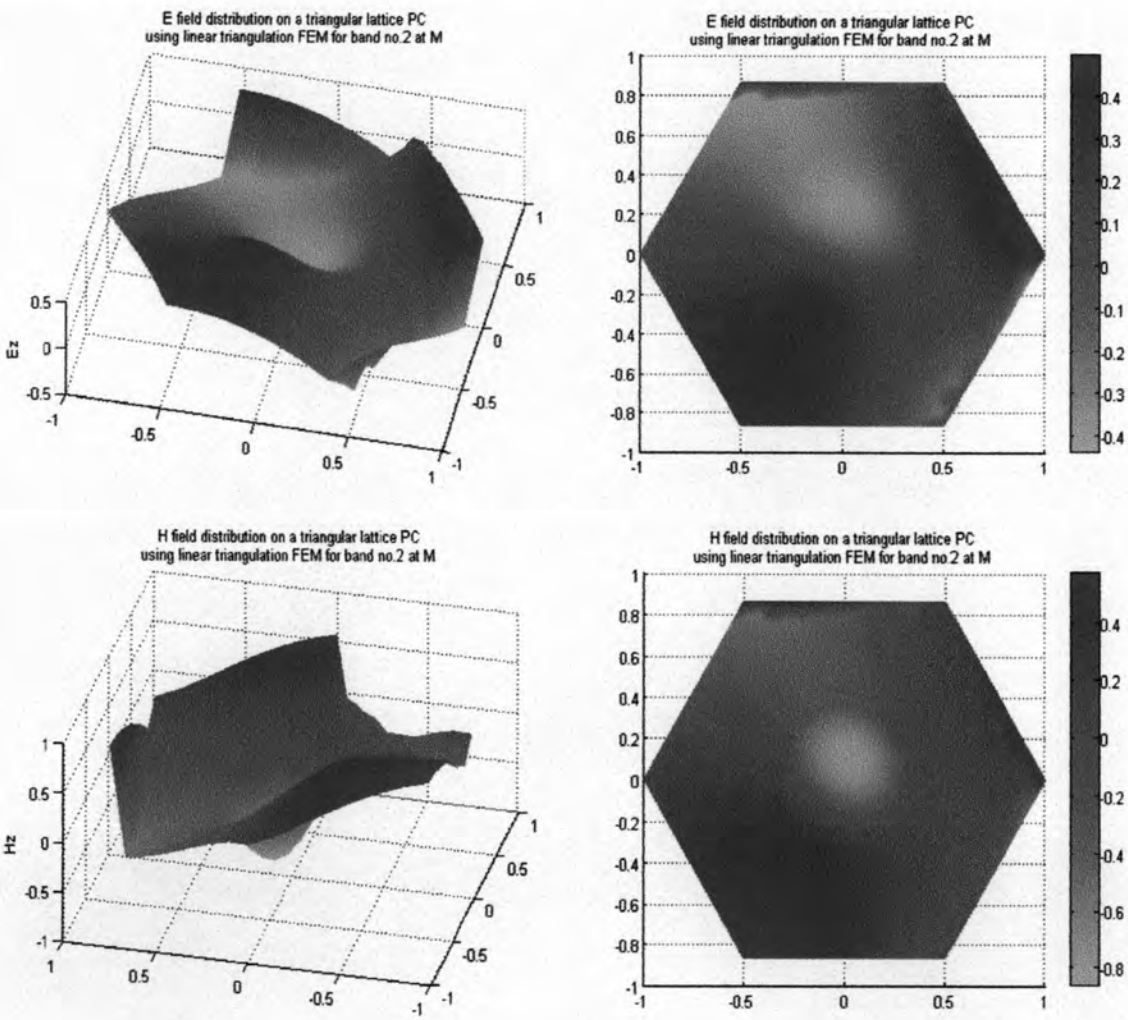

Figure A.14 *E*-field and *H*-field distributions at M point for the second band

At M_3:

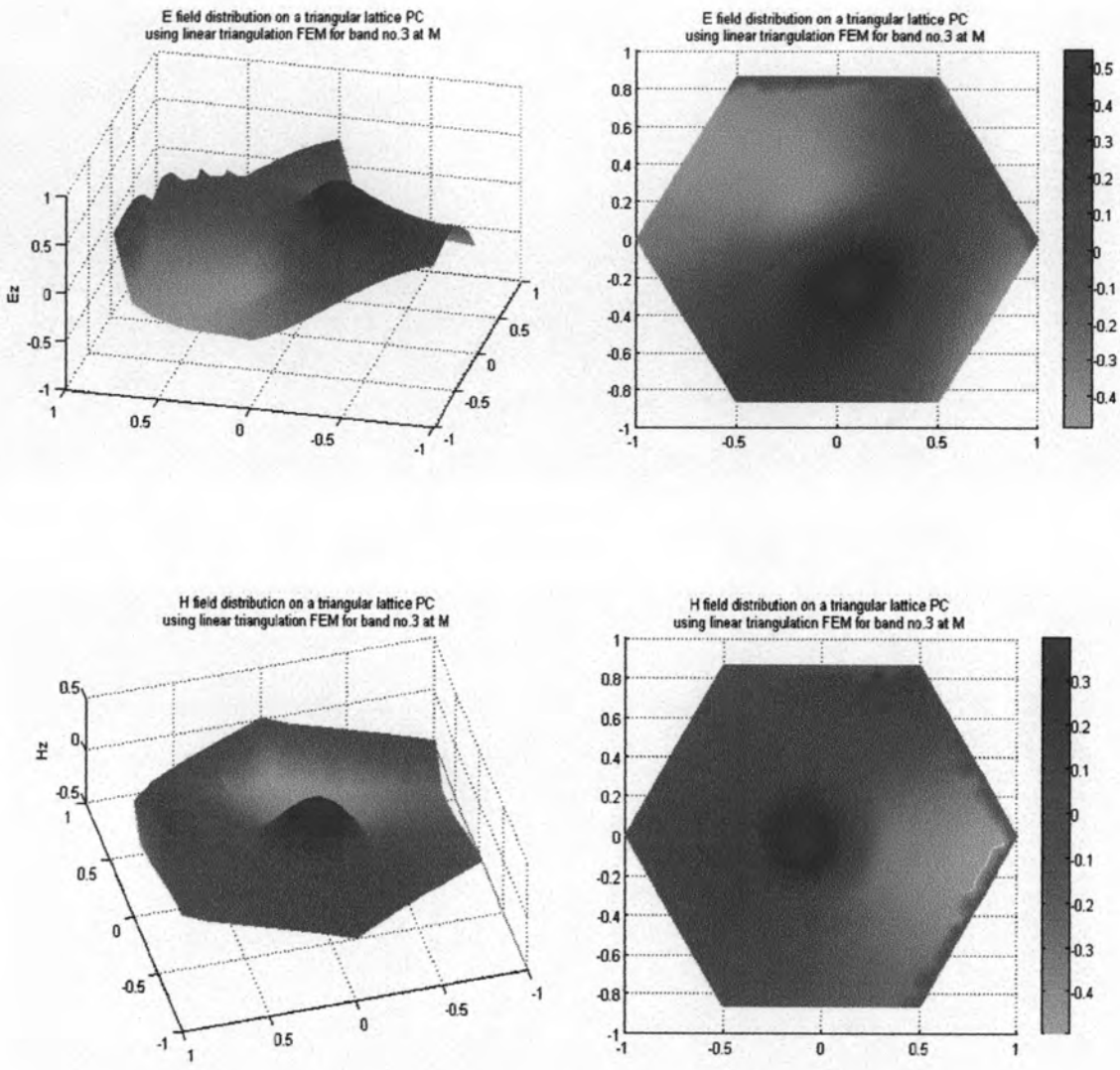

Figure A. 15 E-field and H-field distributions at M point for the third band

APPENDIX B

POLYGONAL MESHES

B.1 Polygonal meshes with n=4 elements

Polygonmesh1*: Num node = 177 Num ele = 156 error_tm = 0.04070195562184 error_te = 0.04062298229192 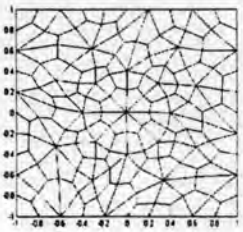	Polygonmesh2*: Num node = 199 Num ele = 178 error_tm = 0.03516589860423 error_te = 0.03530942978373 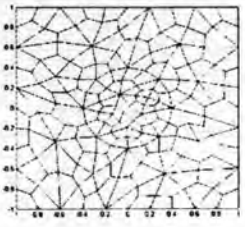
Polygonmesh3: Num nodes = 259 Num ele = 238 error_tm = 0.03845965683624 error_te = 0.03850084620711 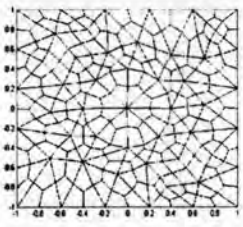	Polygonmesh4*: Num nodes = 273 Num ele = 252 error_tm = 0.03224390432899 error_te = 0.02988495884597 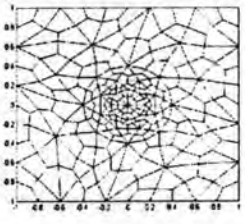
Polygonmesh5: Num nodes = 281 Num ele = 260 error_tm = 0.03330217726566 error_te = 0.03355432540183 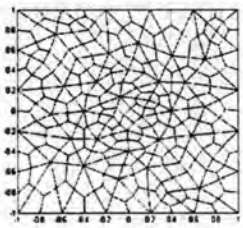	Polygonmesh6*: Num nodes = 355 Num ele = 334 error_tm = 0.03072202366136 error_te = 0.02843700899459 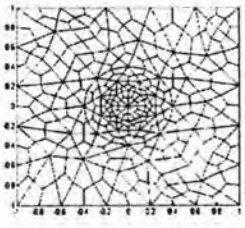
Polygonmesh7: Num nodes = 503 Num ele = 478 error_tm = 0.03701971065089 error_te = 0.03682803743946 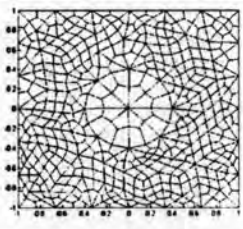	Polygonmesh8: Num nodes = 525 Num ele = 500 error_tm = 0.03209651964504 error_te = 0.03211833953089 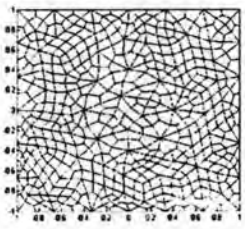
Polygonmesh9: Num nodes = 599 Num ele = 574 error_tm = 0.02981161393905 error_te = 0.02738590395972 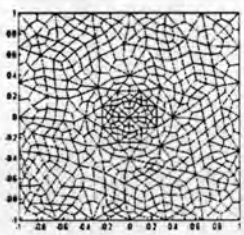	Polygonmesh10*: Num nodes = 739 Num ele = 714 error_tm = 0.02702477785317 error_te = 0.02431476423740 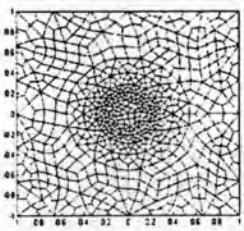

Polygonmesh11*: Num nodes = 997 Num ele = 964 error_tm = 0.02694972936038 error_te = 0.02417000664411 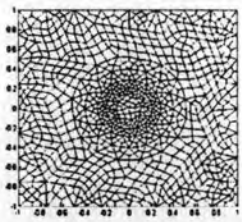	Polymesh 12: Num nodes = 1605 Num ele = 1572 error_tm = 0.02655604475192 error_te = 0.02365279641461 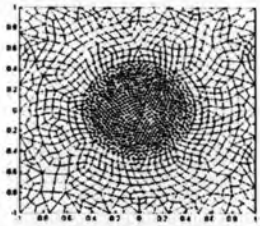

B.2 Polygonal mesh with hybrid elements

Mixmesh1* Num node = 169 Num ele=164 error_tm = 0.04620946006556 error_te = 0.04681188408175 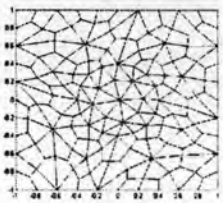	Mixmesh 2* Num nodes = 171 Num ele = 168 error_tm = 0.04222737895124 error_te = 0.04411658252973 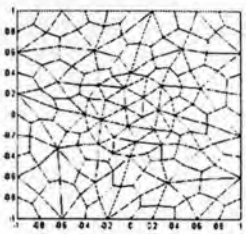
Mixmesh 3* num node = 207 Num ele = 240 error_tm = 0.03340720770209 error_te = 0.03176884039315 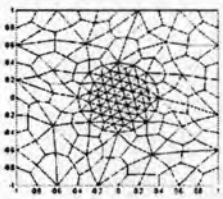	Mixmesh 4 * Num nodes = 234 Num ele = 294 error_tm = 0.03242758363309 error_te = 0.03046656789282 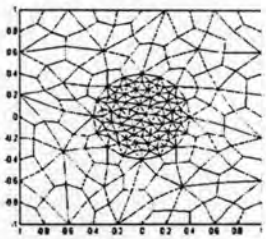
Mixmesh5 Num. node =251 Num. element =246 error_tm = 0.04358299369472 error_te = 0.04446900225910 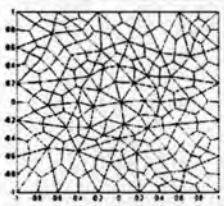	Mixmesh 6 Num. node = 253 Num. element = 250 error_tm = 0.03993133373958 error_te = 0.04183764467310 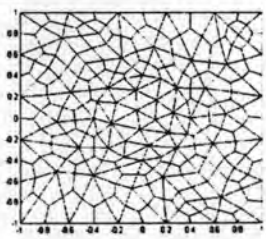
Mixmesh 7 Num. node = 289 Num. element = 322 error_tm = 0.03177216755236 error_te = 0.03017298332058 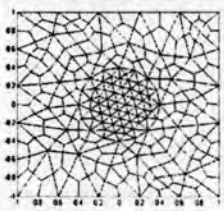	Mixmesh 8* Num. node = 316 Num. element = 376 error_tm = 0.03090322855920 error_te = 0.02896367814389 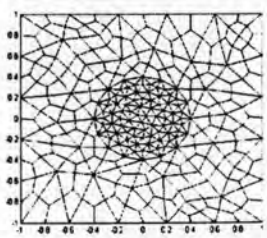

Mixmesh 9
Num. nodes = 348
Num. element = 522
error_tm =
0.03128016050625
error_te =
0.02890661468283

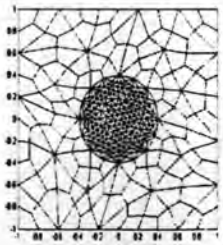

Mixmesh10*
Num. node = 430
Num. element = 604
error_tm =
0.02987562694036
error_te =
0.02753896697416

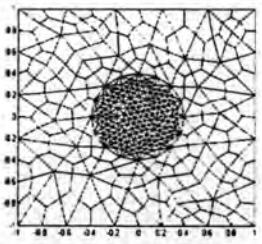

Mixmesh 11
Num. node= 495
Num. element = 486
error_tm =
0.04198299412330
error_te =
0.04240303201002

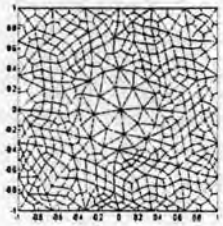

Mixmesh12
Num. node = 497
Num. element = 490
error_tm =
0.03824996144429
error_te =
0.03992054640323

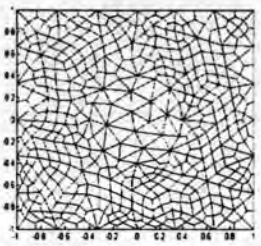

Mixmesh 13
Num. node= 533
Num. element = 562
error_tm =
0.03070023515057
error_te =
0.02896380631636

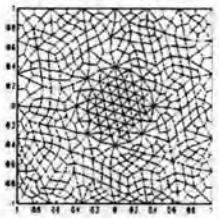

Mixmesh 14
Num. nodes= 560
Num. element = 616
error_tm =
0.02994845291889
error_te =
0.02785639976600

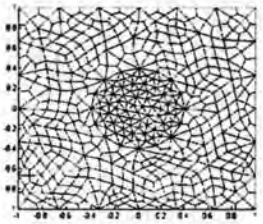

Mixmesh 15*
Num. node = 624
Num. element = 766
error_tm =
0.02763605346311
error_te =
0.02486194831229

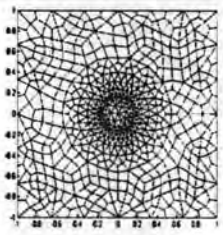

Mixmesh 16
Num. node = 674
Num. element = 844
error_tm =
0.02904630553779
error_te =
0.02656538657543

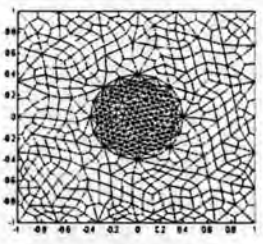

Mixmesh 17*
Num. node = 692
Num. element = 702
error_tm =
0.02705500343367
error_te =
0.02435197635422

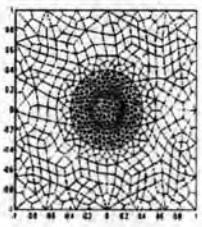

Mixmesh 18
Num. node = 882
Num. element= 1016
error_tm =
0.02752837338314
error_te =
0.02468599492984

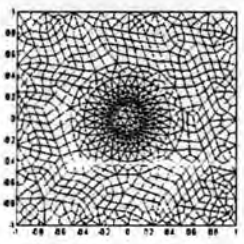

Mixmesh 19*
Num. node = 950
Num. element= 1152
error_tm =
0.02698698883181
error_te =
0.02420424572461

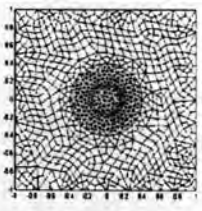

APPENDIX C

FIELD DISTRIBUTIONS OF NON-IDEAL SQUARE 2D PCs

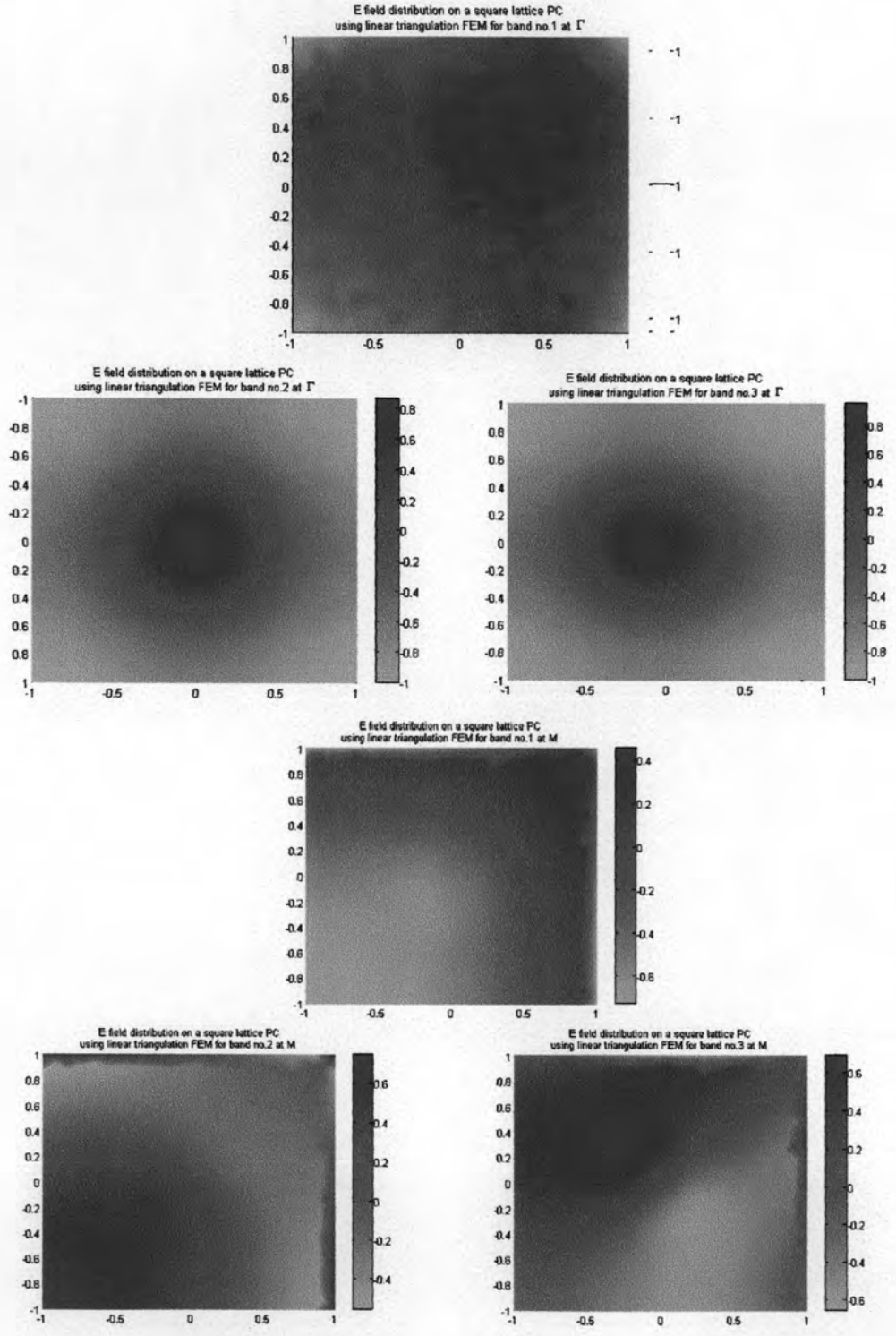

Figure C.1 *E*-field distribution

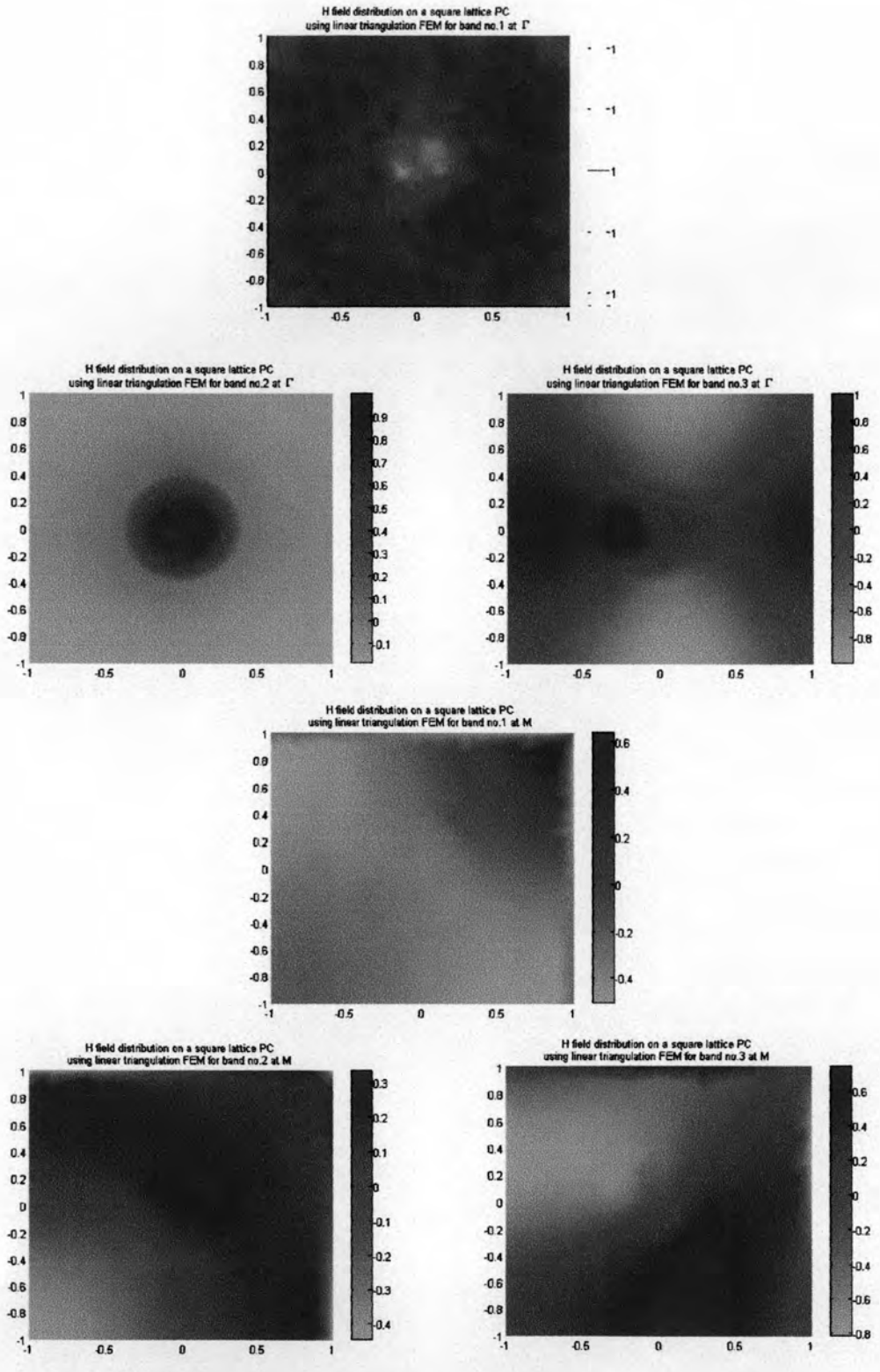

Figure C.2 *H*-field distribution

BIOGRAPHY

Eny Sukani Rahayu received her bachelor degree in electrical engineering from Gadjah Mada University, Yogyakarta, Indonesia, in Mei 2004. Since 2005, she joined the faculty of Gadjah Mada University. In April 2005, she received a scholarship from the AUN/SEED-Net to continue her study at Graduate School of Engineering, Faculty of Engineering, Chulalongkorn University and finished her Master Degree in April 2007. Her research topic interests include photonic crystal, optical systems, and numerical analysis.